IRAQI JOURNAL OF APPLIED PHYSICS
Vol. 22, No. 3, July-September 2026, pp. 462-472

Ahmad A. Hasan [1]
Bushra A. Hasan [1]
Bushra H. Musa [2]
Khaleel I. Hassoon [2*]

[1] Department of Physics, College of Science, University of Baghdad, Baghdad, IRAQ
[2] College of Applied Sciences, University of Technology, Baghdad, IRAQ
* Corresponding author email: khaleel.i.hassoon@uotechnology.edu.iq

Influence of Lithium Salts on Optical Properties, FTIR Analysis, and AC Conductivity of PVP/PVA Blends for Solid Polymer Electrolyte Applications

Blends of polyvinyl pyrrolidone (PVP) and polyvinyl alcohol (PVA) in equal weight ratios (50 wt.% PVP + 50 wt.% PVA) were doped with 15% of various lithium salts (Li_2CO_3, $LiNO_3$, $Li_2SO_4H_2O$, and LiCl) and prepared using the solution-casting method, with dimethylformamide (DMF) as the solvent. The impact of these salts on the blends was analyzed and the results showed that the energy gap was decreased by adding lithium salts Li_2CO_3, $LiNO_3$ and $Li_2SO_4.H_2O$. The minimum energy gap value was 3.5 eV obtained from PVP/PVA:15% Li_2CO_3. The optical constants were determined in the range of 300-1100 nm. The results showed that all the optical constants for doped blends were grown with the addition of lithium salts. The FTIR study confirms the complex formation between the polymer and salt. The present study showed the highest ionic conductivity at room temperature was 2.17×10^{-5} S/cm correspond to PVP/ PVA:15 % Li_2CO_3.

Keywords: PVP/PVA blend; Lithium salts; Optical properties; Dielectric properties
Received: 18 October 2025; Revised: 19 January 2026; Accepted: 26 January; Published: 1 July 2026

1. Introduction

Many research efforts have presently been focused on developing materials for rechargeable batteries. Solid polymer electrolytes (SPEs) represent one of the materials which attract the interest of many researchers because of their potential applications in solid-state high energy density batteries, chemical sensors, solar cells, and electrolyte gate transistors [1-3]. Over time, SPE research has advanced through multiple phases, leading to the development of plasticized, gel, and composite electrolyte systems. Among polymer matrices, polyvinyl pyrrolidone (PVP) and polyvinyl alcohol (PVA) have gained considerable attention due to their environmental stability, moderate electrical conductivity, and excellent processability [4-6]. Their miscibility in all ratios and water solubility make them suitable for various applications. Additionally, PVA is widely employed in multilayer coatings for organic solar cells due to its high transparency and oxygen barrier properties [6-8]. The electrical and optical properties of polymer electrolytes are strongly influenced by doping agents, preparation techniques, and material structure [5,7,8]. Polymers for solid polymer electrolytes applications are often doped with inorganic salts, such as transition metals, to modify their properties, enhancing both conductivity and optical behavior. During the late 1990s, the majority of commercial lithium batteries were fabricated with Li^+-salt solution as electrolytes immobilized in a variety of polymer matrices [9-11]. Researches over the past few years has explored various dopant effects on PVP/PVA blends. For instance, Heiba et al. [12] investigated the electrical and optical behavior of PVP/PVA blends with $ZnCO_2O_4$/CdS nanocomposites, while Ragab et al. [13] performed spectroscopic studies on nickel chloride-doped PVP/PVA blends. Similarly, studies on polymer blend films doped with V_2O_5 nanoparticles composites [14], $CuSO_4$ [15] and $NiCl_2$/$CdCl_2$ [16], have provided insights into their structural and dielectric modifications. However, despite extensive literature on PVP/PVA blends and their dopants, studies on the influence of lithium salts remain limited. Electrochemical devices, particularly energy storage systems, have long relied on liquid electrolytes (LEs). However, due to their volatility and flammability, alternative solid-state electrolytes have garnered significant research interest as safer, more environmentally friendly replacements. Lithium-based SPEs are especially promising due to their potential for efficient ion-transport mechanisms. While prior studies have assessed individual lithium salts' effects on PVP/PVA blends, a comprehensive analysis comparing multiple lithium salts and their impact on both electrical and optical properties remains lacking [17-20]. In the literature, often the effect of only one lithium salt on the electrical or the optical properties on the blend of PVP/PVA is studied [21-24]. This study aims to address this gap by investigating the effects of four lithium salts (Li_2CO_3, $LiNO_3$, $Li_2SO_4H_2O$, and LiCl) on the electrical and optical properties of PVP/PVA blends. By analyzing UV-visible spectra and dielectric responses, we seek to understand how lithium salt doping alters the optical bandgap and enhances ion transport in SPEs. The strong interface interaction

between inorganic salts and organic polymers suggests that lithium doping may significantly improve material performance. This investigation provides valuable insights into the underlying mechanisms governing PVP/PVA based solid polymer electrolytes.

2. Experimental Procedure

The matrix polymeric materials in the presented study have been PVP polymer with a molecular weight of 90000 g/mole supplied by AVONCHEN limited for chemicals, UK. PVA polymer with a molecular weight of 10000 g/mole provided through BDH chemicals and had a high purity (99.999%) supplied by Middlesex Chemicals, England. On the other hand, lithium carbonates (Li_2CO_3), lithium sulphate ($Li_2SO_4.H_2O$), lithium nitrate ($LiNO_3$), and lithium chloride (LiCl) are supplied by BOH company, and dimethyl formamide (DMF), which is used as a solvent, is supplied by Middlesex Chemicals, UK. To create a homogeneous solution, 1 g of each polymer, PVP and PVA, has been continuously dissolved in 25 ml of DMF for 6 hours at a temperature of 70 °C. Then the solution was poured into a clean petri dish of 5 cm diameter and left to evaporate in a temperature-controlled oven at 50 °C for 48 hours. To obtain PVA/PVP blend samples, films doped with 15 % lithium salts, a constant weight ratio of 15 wt.% from lithium salts (Li_2CO_3, $LiNO_3$, $LiSO_4.H_2O$, and LiCl) were dissolved in 25 ml of DMF solution, and after that, each salt solution was added to the undoped PVP/PVA solution using the same volumes. After that, the dried film has been effortlessly taken out of the petri dish. The thickness of the prepared samples has been measured with a digital Vernier caliper, and results showed that the thickness ranged from 0.15±0.5mm. With the use of a Shimadzu UV/VIS160A double-beam spectrophotometer, transmittance as well as, absorbance measurements were performed in a wavelength range of 190-1100 nm. FTIR measurements are implemented using the Fuse Type Shimadzu FTIR spectrophotometer. Every sample was tested in the wavenumber range of 400-4000 cm^{-1}. The LCR Meter model LCR821, covering a 1 to 200 kHz frequency range, was used to evaluate the dielectric properties. The samples of polymer blends have been placed between a parallel plate capacitor's two electrodes. Figure (1) summarizes the preparation and measurements steps.

3. Results and Discussion

According to band theory, electron transitions in polymers from the top of the valence band to the bottom of the conduction band are primarily responsible for UV absorption. In this work, the spectral range 300-1100 nm is used to measure the optical absorbance in this work. Figure (2) displays the absorbance as a function of wavelength for both doped and undoped PVP/PVA samples. The UV-Visible absorption spectra of PVP/PVA solid polymers electrolytes with various lithium salts, including (Li_2CO_3, $LiNO_3$, $Li_2SO_4.H_2O$, and LiCl) spectra up to 400 nm, decreased with increasing wavelength, while the absorption increased with increasing lithium salts (Li_2CO_3, $LiNO_3$, $Li_2SO_4.H_2O$, and LiCl), However, the values of the absorbance are improved by adding lithium salts. PVP 50%-PVA 50%:15% Li_2CO_3 has maximum absorbance. One can note that the increase in absorbance varies from one salt to another i.e. either polymer blend doped with lithium salts by weight 15%, its absorbance will be higher than the undoped PVP/PVA blend because the doped samples are more opaque than the undoped samples. The incident radiation at the lithium salts ions is combined with the polymer chains, which absorb the shortest wavelengths, as shown in Fig. (2). It is clear from the same figure that the absorption spectra for all composites blends decreased with increasing wavelength while the absorption increased with the addition of lithium salts to the polymer blends. This indicated the formation of charge transfer complexes between the polymer blend and the filler [25].

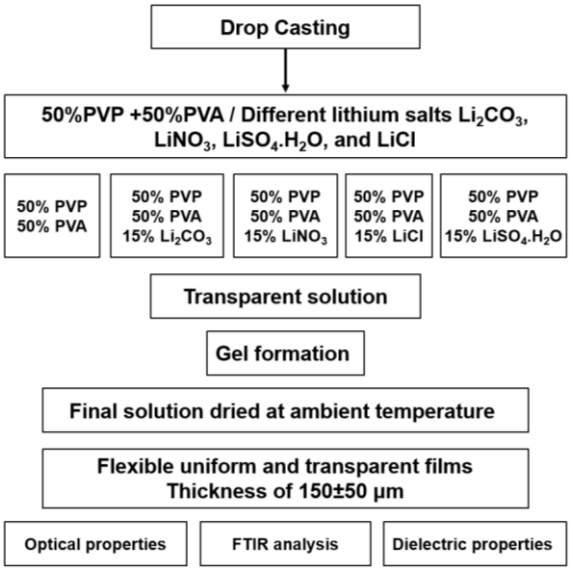

Fig. (1) Flow chart of preparation and characterization steps of PVP/PVA: lithium salts blend polymer electrolytes

The absorption coefficient (α) represents the relative rate at which the intensity of the light decreases. From optical absorption spectra, the absorption coefficient as a function of wavelength α(λ) (cm^{-1}) is calculated using Beer-Lambert's formula [26]:

$$\alpha(\lambda) = 2.303 \frac{A(\lambda)}{t} \quad (1)$$

Here, A is the absorbance (also called the optical density), while the sample thickness is denoted as t

Figure (2) shows that the absorption characteristics of lithium-doped PVP/PVA blend generally display a high absorbance in the UV region due to electronic transitions, such as π-π^* transitions within the polymer's

molecular structure. The enhanced absorbance post-doping is attributed to the interaction of lithium ions with functional groups in PVP and PVA, specifically hydroxyl (−OH) and carbonyl (C=O), resulting in modifications in molecular structure and optical properties. Furthermore, lithium doping augments the amorphous character of the polymer blend, thereby increasing light absorption. Additionally, lithium salts introduce mobile ions, which modify the electronic transitions within the polymer matrix, further elevating absorbance. Lithium doping can slightly shift these transitions, reflecting changes in the electronic environment of the polymer matrix. $LiNO_3$ and Li_2CO_3 shows maximum absorbance compared with LiCl and $Li_2SO_4.H_2O$. As the wavelength increases into the visible region and IR regions, the absorbance gradually decreases, a common trend in many polymeric materials, and any shifts in this range depend on the lithium-ion concentration and its distribution in the polymer blend. Overall, the absorbance-wavelength trends highlight the interplay between the polymer blend and lithium ions, offering useful information for optimizing the material for energy storage or optical applications. Figure (3) illustrates that the absorption coefficient increases with higher energy levels, indicating a higher probability of electron transition for increased photon energy [27,28]. Furthermore, the figure demonstrates that the sample doped with lithium salts exhibits a higher absorption coefficient compared to the undoped blend sample (50 PVP/50 PVA).

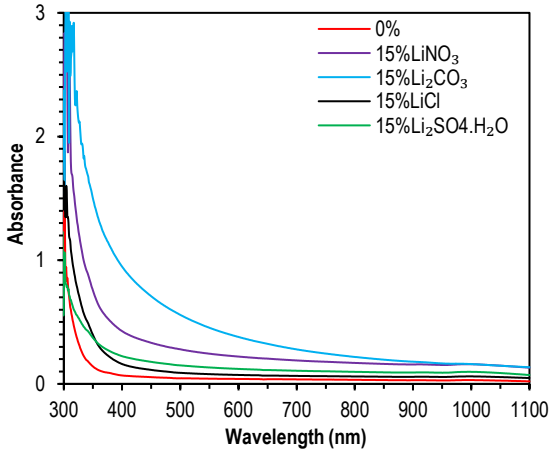

Fig. (2) Absorption spectra of PVP/PVA blends doped with different amounts of lithium salts

The refractive index (n) can be determined using the following equation [29]:

$$n = \frac{(1+R)}{(1-R)} + \sqrt{\frac{4R}{(1-R)^2} - \kappa^2} \qquad (2)$$

where R is the reflectance, and k represents the extinction coefficient which can be determined from the wavelength using the following relationship [26]:

$$\kappa = \alpha\lambda/4\pi \qquad (3)$$

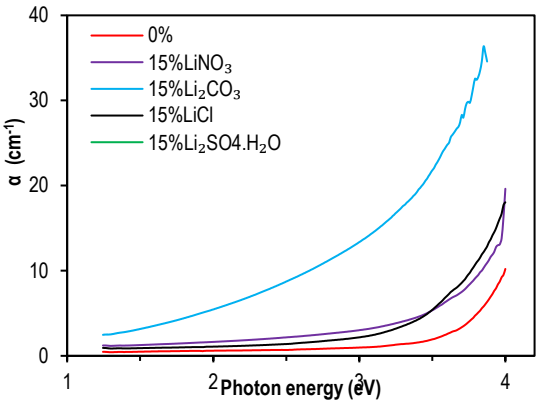

Fig. (3) Variation of absorption coefficient α(λ) with wavelength for PVP/PVA blends doped with different lithium salts

The optical characteristics of a material are significantly influenced by the interactions between incident light waves and the material. Figure (4) shows the wavelength dependent absorbance data for pure and doped blends with Li_2CO_3, $LiNO_3$, $Li_2SO_4H_2O$, and LiCl salts. The absorbance spectrum is prominent in the UV range, but minimal in the visible range. Upon doping the blend with different salts, absorbance changes varied. The absorbance increased slightly with PVP/PVA:Li_2NO_3, significantly with PVP/PVA:Li_2CO_3, and decreased with PVP/PVA:$LiSO_4H_2O$ and PVP/PVA:LiCl. The increase in absorbance for PVP/PVA:Li_2CO_3 and PVP/PVA:$LiNO_3$ is attributed to the agglomeration of the salts at the blend surface, indicating different interactions between PVP/PVA molecules and the salts. Higher absorbance in the 300-400 nm range for the doped blends suggests their use as UV shielding materials. These absorbance alterations imply changes in crystallinity, bandgap structure, and refractive index when doping with different salts. The red shift observed in PVP/PVA:$LiNO_3$, PVP/PVA:Li_2CO_3 and PVP/PVA:$LiSO_4H_2O$ indicates a decrease in the optical bandgap due to sub-level formation between the highest occupied and lowest unoccupied molecular orbitals within the host blend matrix.

Figure (4) illustrates the refractive index (n) as a function of wavelength for both undoped and lithium-doped PVP/PVA blends. This figure shows that the doped samples exhibit higher refractive index values compared to the undoped PVP/PVA. For quantitative comparison, the refractive index values at a wavelength of 550 nm are listed in table (1).

Table (1) Refractive index values at wavelength 550 nm for undoped and lithium doped PVP+PVA, where n_0 is the refractive index for undoped PVP/PVA

Sample	n	n/n_0
PVP/PVA	1.23	1
15% LiCl	1.33	1.08
15% $Li_2SO_4.H_2O$	1.44	1.17
15% $LiNO_3$	1.63	1.32
15% Li_2CO_3	1.91	1.55

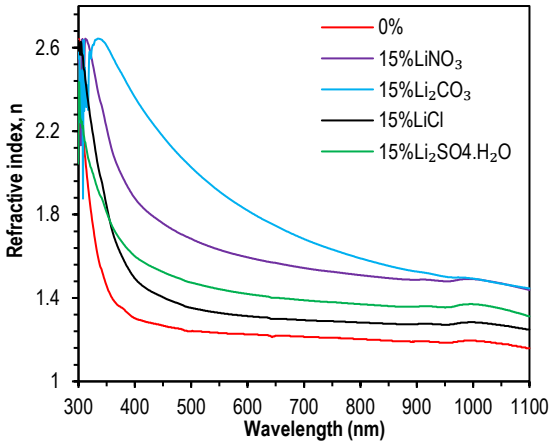

Fig. (4) Variation of refractive index (n) with wavelength for PVP/PVA blends with different lithium salts at room temperature and thickness of 300µm

The data in the table indicates that doping PVP/PVA with Li_2CO_3 results in the greatest relative increase in refractive index (n/n_0=1.55), whereas doping with LiCl results in the smallest relative increase (n/n_0 =1.08). The findings presented by Fig. (4) align with general trends observed in polymer blends, where the refractive index decreases as wavelength increases. A study on PVA/PVP blends doped with different salts reported a refractive index reaching around 3.5 in the 400-800 nm range, depending on the salt concentration. A separate investigation by Farrage et al. [30] into Sb_2S_3+ PVA+PVP nanocomposites showed refractive index variations based on filler content, with optical properties analyzed across 200-2500 nm.

As seen in Fig. (5), the doped samples' extinction coefficient (k) values are higher than the undoped PVP/PVA sample values. The variation of optical properties as a result of lithium salt doping is due to lithium ions interacting with the hydroxyl groups in PVA and the carbonyl groups in PVP, forming coordination complexes. This disrupts the existing hydrogen bonding network within the polymer blend, leading to changes in the electronic environment. These interactions modify the polymer's microstructure, increasing the amorphous regions, which are more optically active. This enhances light absorption and increases the absorption coefficient. Moreover, the incorporation of lithium salts introduces localized states within the polymer matrix, which can facilitate electronic transitions. This reduces the optical bandgap, allowing the material to absorb light at lower energies (longer wavelengths).

The dielectric constant's real and imaginary parts are represented by the complex dielectric function $\varepsilon=\varepsilon_r+\varepsilon_i$. The expressions for these parts are given below [26]:

$$\varepsilon_r = n^2 - \kappa^2 \quad (4)$$

and

$$\varepsilon_i = 2n\kappa \quad (5)$$

Equation (5) shows that the real part is influenced by the extinction coefficient due to the very small refractive index value. The real part of the dielectric constant (ε_r) is associated with the dispersion of the electromagnetic waves when they move throughout the material, and it is also responsible for the reduction in the propagation speed of the waves throughout the blend. Furthermore, the imaginary part (ε_i) represents the energy absorption from the electric field due to dipole movement; consequently, it gives a measure of the disruptive rate of the wave in the blend [31-32]. The wavelength dependence of the ε_r and ε_i values of all blends is shown in figures (6) and (7).

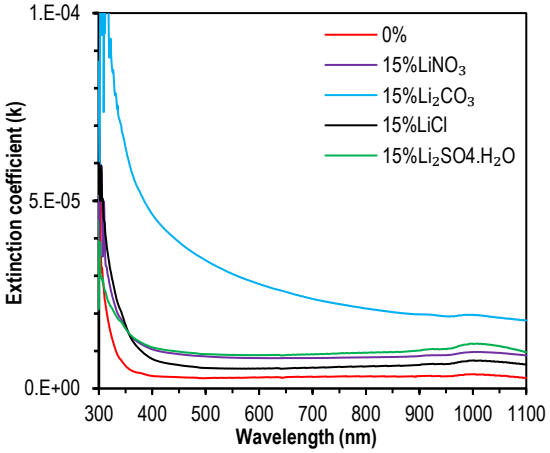

Fig. (5) Variation of extinction coefficient (k) with wavelength for PVP/PVA blends doped with various lithium salts at room temperature, thickness of 300µm

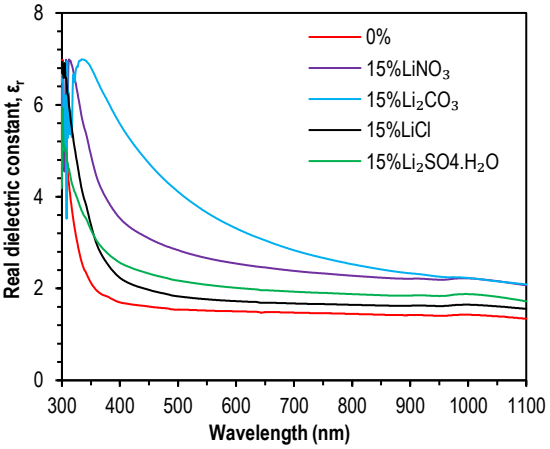

Fig. (6) Variation of real dielectric constant (ε_r) with wavelength for PVP/PVA blends doped with various lithium salts at room temperature, thickness of 300µm

In each blend, the values of ε_r are greater than the value of the corresponding ε_i. This is because the values of ε_r are strongly correlated with the n value, whereas the values of ε_i are based on k values. In the visible range, the ε_r and ε_i values increased by doping with Li_2CO_3 and $LiNO_3$ salts. The highest ε_r and ε_i values were obtained as the PVP/PVA blend was doped with 15% Li_2CO_3. The changes in the dielectric constants

with the incident photon energy demonstrated that there are some interactions that take place between the incident photons and the free electrons in the studied range.

The absorption coefficient can be calculated from the Urbach's energy as follows [33,34]:

$$\alpha = \alpha_0 \exp(\frac{hv}{E_u}) \quad (6)$$

where E_u is the Urbach energy and α_0 is a constant. One could obtain Urbach energy from the inverse of slope for ($\ln\alpha$) vs. photon energy (hv)

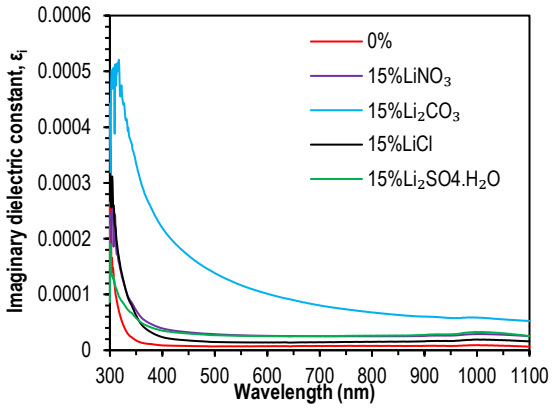

Fig. (7) Variation of imaginary dielectric constant (ε_i) with wavelength for PVP/PVA blends doped with various lithium salts at room temperature, thickness of 300µm

Figure (8) and table (2) show that doping the blend of PVP/PVA with different lithium salts increases the value of Urbach energy. This trend can be attributed to the rising defect levels in the bandgap resulting from doping with various lithium salts [34]. Table (2) presents Urbach energy values. Based on Tauc's relationship [34], the relationship between energy bandgap and absorption coefficient is given by:

$$(\alpha hv) = B\,(hv\text{-}E_g)^r \quad (7)$$

where B is a constant that varies with the transition type and aids in material diagnostics, E_g is the optical bandgap energy, while hv is the photon energy

The index r refers to the electronic transition type, with values of 1/2, 3/2, 2, or 3 for allowed and forbidden direct and indirect transitions. The plot of $(\alpha hv)^2$ *vs.* photon energy (hv) determines direct bandgap values. Figure (9) shows the direct bandgap values for 50 PVP/50 PVA, obtained by extrapolating the straight line to $(\alpha hv)^2 = 0$. Optical energy gap for PVA/PVP blends undoped and doped with different lithium salts were obtained from plot the relation between $(\alpha hv)^{1/r}$ as a function of photon energy on drawing a straight line from the upper part of the curve toward the (x) axis. The energy gap was obtained for the allowed indirect transition. The obtained values are shown in table (2). It can be seen that the values of the energy gap reduced by adding $LiNO_3$, Li_2CO_3, and $Li_2SO_4.H_2O$ lithium salts. Indeed, the energy gap reduced from 3.8 to 3.7, 3.5 and 3.7 eV, respectively. The effect of adding Li_2CO_3 salt among the salts to the polymer blends is more pronounced than $LiNO_3$ and $Li_2SO_4.H_2O$. The shift of the energy gap to the low energy side is attributed to the creation of onsite levels in the energy gap. The transition, in this case, is conducted in two stages that involve the transition of an electron from the valence band to the local levels [35]. The minimum optical energy gap (3.5 eV) was obtained for blend sample (PVP/PVA) doped Li_2CO_3 as shown in table (2).

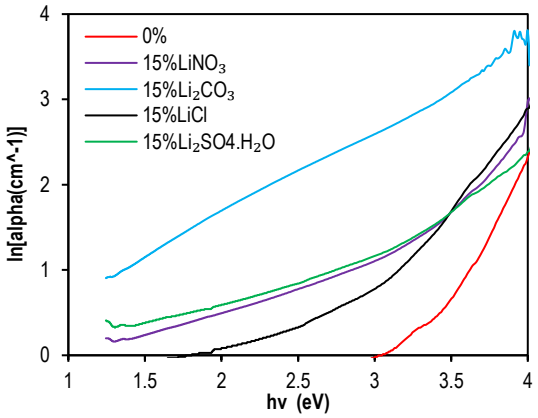

Fig. (8) Variation of ln(α) with photon energy (hv) for PVP/PVA blends doped with different lithium salts

The inverse relationship between Urbach energy (or the depth of localized states) and the energy bandgap is clearly observed from table (2). The lowest value of the energy gap corresponds to the maximum value of Urabch energy which is achieved for PVP/PVA:15%$LiCO_3$. This sample has the highest electrical conductivity as seen in the next section.

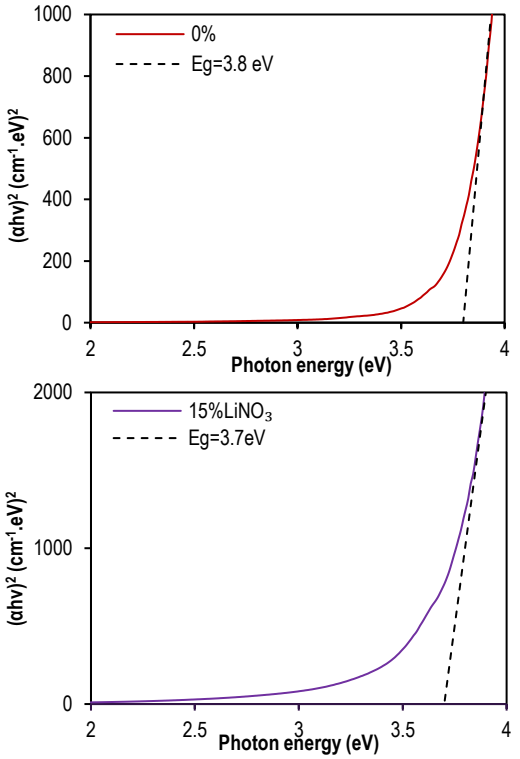

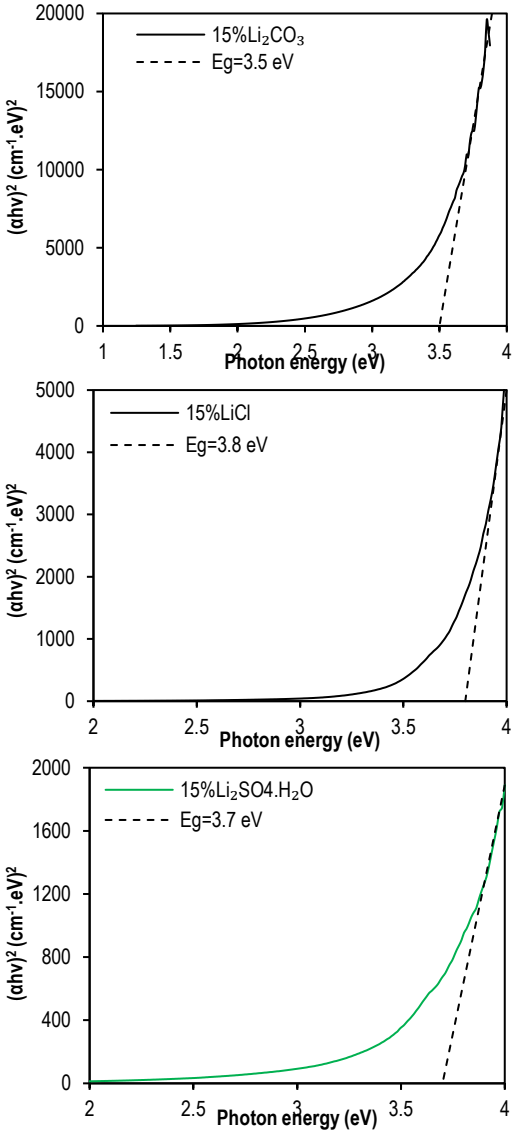

Fig. (9) Variation of $(\alpha h\nu)^2$ with photon energy ($h\nu$) for PVP/PVA blends doped with different lithium salts

Figures (10) and (11) show FTIR absorption spectra of PVP/PVA undoped and doped with various lithium salts at room temperature in the region 4000-400 cm^{-1}. The spectra exhibit bands characteristic of stretching and bending vibrations of the films. From the spectra, for pure PVA, the broad band at about 3500 cm^{-1} is assigned to O–H stretching vibration of hydroxylgroup. The band corresponding to CH_2 asymmetric stretching vibration occurs at about 2935 cm^{-1}. The band at about 1039 cm^{-1} corresponds to C–O stretching of acetyl groups presenting the PVA backbone. The vibrational band at about 1658 cm^{-1} corresponds to C=O stretching of PVA and PVP [36,37]. The appearing of C=O stretching is due to semi-crystalline nature of the blends. In case of PVA/PVP dope with lithium salts, FTIR spectra shows shifts in some bands and change in the intensities of other bands comparing with pure films. This indicates the considerable interaction between the polymers and Li-ions.

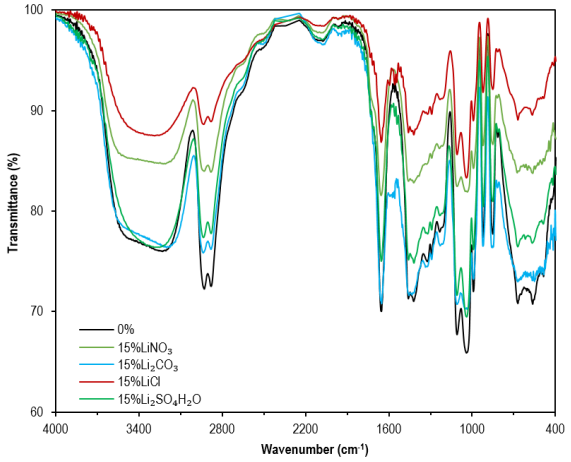

Fig. (10) FTIR spectra of 50%PVP/50%PVA undoped and doped with different lithium salts

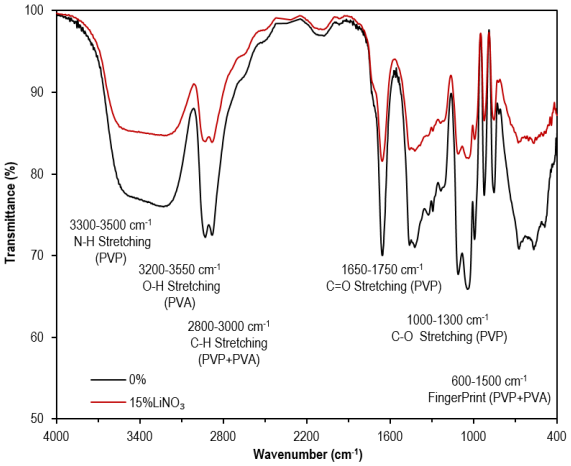

Fig. (11) FTIR spectra of 50%PVP/50%PVA undoped and doped with lithium salt (15%$LiNO_3$)

From the FTIR spectrum, it is clear that the Li_2CO_3-doped PVA/PVP sample declared lowest transmittance, i.e., highest absorbance in compared with pure and other doped samples. The spectra of doped PVA/PVP blend doped with various lithium salts shows that the peak in the wavelength range 3200-3500 cm^{-1} of (OH) stretching is broader for PVA/PVP doped with Li_2CO_3, $LiNO_3$ and become narrower for PVP/PVA samples doped with $Li_2SO_4.H_2O$ and LiCl. Also, the intensity of C=O peak (~1658 cm^{-1}) for doped samples is lower than the undoped blend. These confirm that the interaction between the PVP/PVA blend and the lithium salts. The effect of different lithium salts on some characterizing IR bands can be taken as a measure of structural changes of PVP/PVA blend due to the filling. It is known that the wavenumber shifts of IR bands evidence the change in the potential energy distribution along the polymeric chain due to the filling.

For more explanation, when lithium salts are added to the PVP/PVA polymer blend, significant changes in

the FTIR peaks occur due to complexation and hydrogen bonding interactions. Notable changes include [38-40]: (i) the C-H peak shifts from 800.45 to 798.52 cm^{-1}, (ii) the acetyl (C-O) stretching bond shifts from 850.60 to 846.75 cm^{-1} when doped with LiCl, (iii) the C-N stretching band shifts from 1290.3 to 1288.4 cm^{-1} with $LiNO_3$ doping, and (iv) the C=O stretching bond shifts from 1707 to 1650 cm^{-1} due to pyrrolidone rings. The key FTIR features include: (i) O-H stretching (3200-3550 cm^{-1}), broad peaks indicating hydroxyl groups, associated with hydrogen bonding in polymers like PVA, (ii) N-H stretching (3300-3500 cm^{-1}) corresponding to amine groups in PVP, (ii) C-H stretching (2800-3000 cm^{-1}), characteristic of aliphatic hydrocarbons in both PVP and PVA, (iv) C=O stretching (1650-1750 cm^{-1}), strong peak due to the carbonyl group in PVP, (v) C-O stretching (1000-1300 cm^{-1}) associated with ether or alcohol groups in PVA, and (vi) fingerprint region (600-1500 cm^{-1}) contains unique peaks for identifying specific molecular structures. These features are depicted in Fig. (11) for undoped and 15%$LiNO_3$ doped PVP/PVA blends.

The active bonds are as follows: (i) C-N stretching, shift from 1290.3 to 1288.4 cm^{-1} with $LiNO_3$ doping, (ii) C=O stretching, shift from 1707 to 1650 cm^{-1} due to pyrrolidone rings, (iii) hydroxyl (-OH) groups, shifts in the broad absorption band around 3200-3500 cm^{-1} suggest hydrogen bonding alterations due to lithium-ion coordination, (iv) carbonyl (C=O) groups, the peak near 1650 cm^{-1} shifts due to complexation between lithium ions and PVP's carbonyl groups, (v) C–O–C stretching, changes in the 1100-1300 cm^{-1} region indicate modifications in polymer backbone interactions, and (vi) SO_4^{-2} and NO^{-3} effects, lithium sulfate and lithium nitrate introduce additional peaks related to their respective anions, affecting polymer bonding.

Equation (8) can be used to determine the real dielectric constant (ε_r), based on the sample's measured capacitance [41-43]:

$$\varepsilon_r = C_p d/\varepsilon_0 A \quad (8)$$

where d, ε_0 and C_p is the sample thickness, free space permittivity, and capacitance respectively. The imaginary dielectric constant (ε_i) can be deduced from the following relation

$$\varepsilon_i = \sigma_{a.c}/\varepsilon_0\omega \quad (9)$$

while the loss tangent ($\tan\delta$) is measured thought the relation

$$\varepsilon_r = \varepsilon_i tan\delta \quad (10)$$

The addition of various amounts of lithium salts on undoped PVP/PVA blend characteristics is shown by dielectric permittivity as a function of frequency. Figures (12) displays frequency-dependent ε_r for PVP/PVA blend samples doped with different lithium salts. This behavior is typical for polymer electrolytes and can be attributed to dielectric dispersion. At lower frequencies, the material's dielectric constant is high due to electrode polarization and the ability of dipoles to align with the applied electric field. As the frequency increases, the dipoles fail to respond quickly to the oscillating field, leading to a drop in the dielectric constant. Doping with lithium salts enhances ionic conduction, contributing further to the dielectric properties, especially at lower frequencies where conductivity effects dominate. The figure illustrates that PVP/PVA doped with Li_2CO_3 and $Li_2SO_4H_2O$ have higher ε_r than other lithium salts. Figure (6) clearly demonstrates that the dielectric constant of the polymer blend varies significantly depending on the type of lithium salt used.

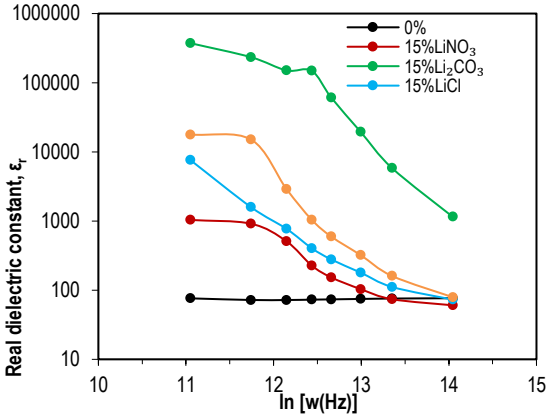

Fig. (12) Frequency dependency of ε_r for PVP/PVA blend doped with various lithium salts

The dielectric constants of polymers doped with Li_2CO_3 and $LiSO_4{\cdot}H_2O$ are notably higher compared to those doped with LiCl and $LiNO_3$. This disparity can be attributed to several key factors [44-46]: (a) ion size and polarizability, as larger anions such as CO_3^{2-} in Li_2CO_3 and SO_4^{2-} in $Li_2SO_4{\cdot}H_2O$ contribute to higher polarizability, enhancing the dielectric constant, (b) stronger polymer-salt interactions, as these salts form robust hydrogen bonds and ionic interactions with PVP and PVA, leading to increased dipole alignment and dielectric response, (c) water content influence, as the hydration water in $Li_2SO_4{\cdot}H_2O$ enhances charge mobility, thereby improving dielectric properties. The hydration water presence in PVP/PVP undoped and doped with various lithium salts samples, and in particular the PVP/PVP doped with $Li_2SO_4{\cdot}H_2O$ sample, has been observed by other researchers. Abdelrazek [4] pointed out from the TGA thermograms of weight loss as a function of temperature for pure PVP/PVP blend and their complexes that, the initial weight loss for all the samples occurs at 75±2 °C due to the moisture evaporation and it is stable up to 135±3 °C, above which the solvent evaporated. The major weight losses are observed in the range of 233-463 °C for all the prepared samples. This may be correspondent to the structural decomposition of the polymer blends and their complexes. They added that the prepared samples are stable over 463 °C and are preferred in lithium polymer batteries. The last effect is (d)

crystallinity reduction, as lithium carbonate and sulfate increase the amorphous nature of the polymer blend, which positively impacts dielectric behavior. In contrast, LiCl and $LiNO_3$, with their smaller anions (Cl^- and NO_3^-), exhibit lower polarizability, resulting in diminished dielectric constant values.

Figure (13) reveals the behavior of the imaginary dielectric constant (ε_i) against frequency for PVP/PVA polymer blends doped with different Lithium salts. The imaginary part of the dielectric constant, which is linked to the dielectric loss, typically decreases with increasing frequency. At lower frequencies, the imaginary part is higher due to significant energy dissipation caused by charge carrier motion, electrode polarization, and other relaxation processes. As the frequency rises, these processes can't keep up with the oscillating electric field, resulting in reduced energy losses and a subsequent drop in the imaginary dielectric constant. The incorporation of lithium ions can influence this trend, as their mobility contributes to ionic conduction and dielectric losses, particularly at lower frequencies [49]. Here Li_2CO_3 gave maximum values for ε_i. It is noteworthy that in polar materials, initial high ε_i and ε_r values decrease as field frequency increases because dipoles cannot keep up with field fluctuations, leading to reduced ion diffusion and charge-induced polarization. Doped samples consistently show higher ε_i and ε_r values than undoped samples due to polymer/dopant interface polarization and increased accumulated charge. Thus, polymers doped with lithium salts exhibit a larger dielectric constant compared to undoped ones.

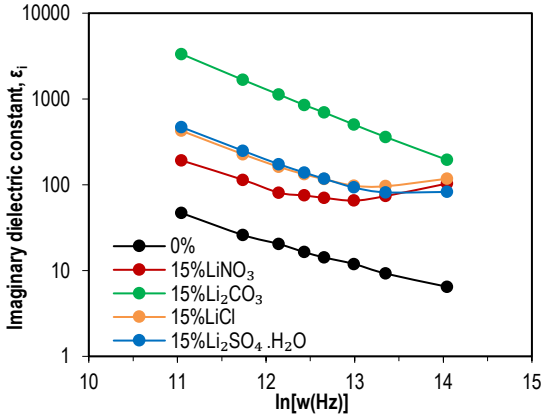

Fig. (13) Frequency dependency of ε_i for PVP/PVA blend that has been doped with various lithium salts

In general it can noticed for each sample, ε_i and ε_r decrease with increasing frequency, starting high at low frequencies and eventually stabilizing at higher frequencies. The C_p and tanδ for each sample are measured within a 1–200 kHz range of frequency.

Figures (14) and (15) show the effect of doping a PVP/PVA blend with various lithium salts on C_p and tanδ. It can be observed from Fig. (13) that C_p showed irregular variation with doping with various salts, it revealed increasing with doping with Li_2CO_3 and $LiNO_3$ while the opposite to that was take place with doping by residual salts. Except for LiCl, which is found to decrease, the values of tanδ have been observed to increase with the addition of lithium salts, i.e., the values of tanδ of doped samples are exceeded that of undoped one except the LiCl doped PVP/PVA sample with which shoes drastic decrease in compare with undoped samples.

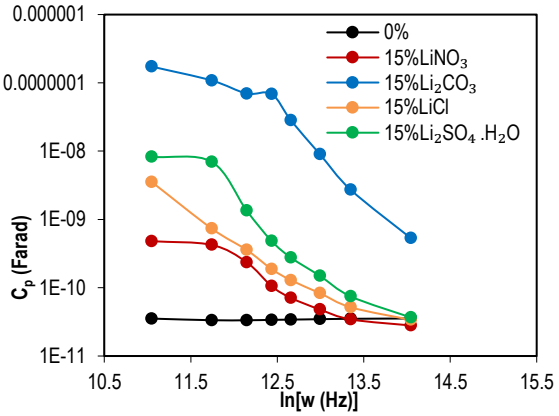

Fig. (14) The relationship between C_p and lnω for PVP/PVA blend doped with different lithium salts

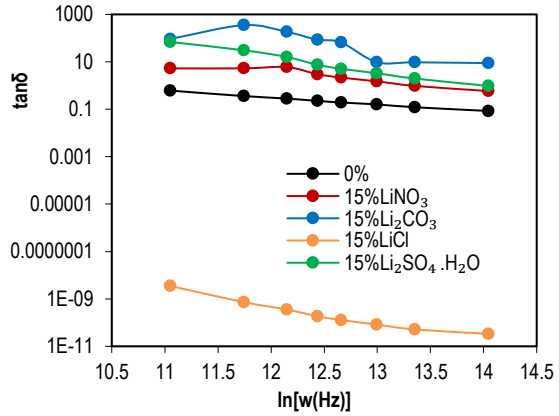

Fig. (15) Correlation between tanδ and lnω for PVP/PVA blend doped with different lithium salts

The logarithmic plot of the variation of conductivity as a function of the angular frequency for the 50 PVP/50 PVA blend with different lithium salt polymer blend electrolyte complex at 303 K is shown in Fig. (16). As seen from this figure, the frequency-dependent conductivity plot shows two distinct regions. The first region with low-frequency dispersion is for dc conductivity. The second region is formed due to oscillating charges at higher frequencies. In this study, the frequency dependent conductivity spectra is analyzed using Jonscher's power law [50]

$$\sigma(\omega) = \sigma_{ac} + A\omega^s \qquad (11)$$

Ac conductivity may be obtained using the following equation [51]:

$$\sigma_{ac} = \frac{d}{R_b.A} \qquad (12)$$

where d is thickness of sample, A is the effective area, and R_b is the resistance. Frequency dependency of σ_{ac} could be found using the following equation to study the primary conduction mechanism.

$$\sigma_{ac} = A\omega^s \quad (13)$$

where A, ω and s are constant, angular frequency, exponential power, respectively

In the high-frequency region, conductivity increases with the frequency. The mobility of charge carriers is higher in the high frequency region [42]. Numerous studies confirm the presence of significant ionic conductivity in PVP/PVA blends doped with lithium salts. This phenomenon is central to their application as solid polymer electrolytes in various energy storage devices like lithium-ion batteries. The movement of lithium ions is highly coupled with the dynamic segmental motion of the amorphous polymer chains. The ions "hop" between temporary coordination sites within the free volume of the polymer matrix.

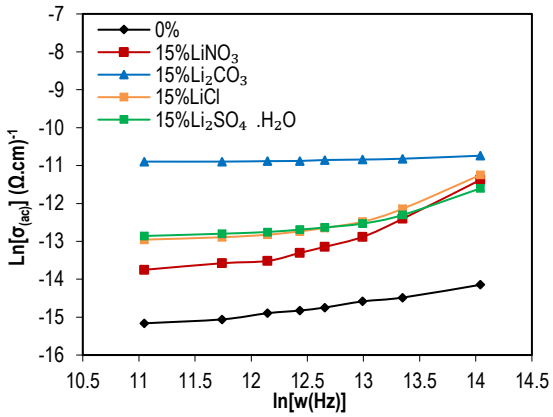

Fig. (16) ln(σ_{ac}) as a function of lnω for PVP/PVA blend that had been doped with different lithium salts

The addition of the lithium salt increases the number of mobile charge carriers (Li^+ ions) available for conduction. The reported ionic conductivity values for PVP/PVA lithium-doped systems generally fall within the range of 10^{-8} to 10^{-6} S/cm at room temperature, depending on the specific salt (e.g., lithium acetate, lithium bromide, lithium perchlorate, lithium nitrate), concentration, and the potential addition of plasticizers or nanofillers. In this work, the highest ionic conductivity 2.15×10^{-5} S/cm has been observed for the composition of 50 PVA/50 PVP:15% Li_2CO_3, this results agree with the findings of many researches as in references [52-57]. The effect of lithium salts on PVP/PVA on dielectric constant can be explained as follows: The presence of lithium ions introduces mobile charge carriers into the polymer's matrix. These ions move through the blend regions via mechanisms like hopping and vehicular transport, leading to improved ionic conductivity. Moreover, lithium ions enhance the dielectric constant of the blend, which reduces the energy barrier for ion migration. This further supports efficient ion-transport.

Based on the above unique optical and electrical properties, PVP/PVA blends doped with lithium salts can be used in lithium-ion batteries as solid polymer electrolytes, offering high ionic conductivity. Moreover, they can be utilized in electrochemical devices such as smart windows and displays, where their ability to conduct ions facilitates reversible color changes under an applied voltage. Finally, Li-doped PVP/PVA electrolytes offer excellent safety, flexibility, and lightweight properties, making them ideal for applications such as wearable electronics. Solid-state electrolytes promise unmatched safety, durability, and thermal stability, but face challenges such as high production costs and mechanical fragility.

4. Conclusions

PVP- and PVA- based lithium ion conducting polymer electrolytes with 15 wt.% from different lithium salts have been prepared successfully by solution casting technique using DMF as solvent. The addition of lithium salts showed a clear effect on all optical constants values of the PVP/ PVA blend, especially Li_2CO_3, where the highest values were reached for the refractive index, extinction coefficient, and dielectric constant in both its real and imaginary parts. The FTIR provides an evidence for the existence of an interaction between Li^+ ion and polymer thereby revealing the complexation in the prepared polymer electrolytes. From the conductivity analysis, the highest ionic conductivity at room temperature has been found to be 2.17×10^{-5} S/cm for the composition of PVP/PVA:15% Li_2CO_3 which consistent with lowest energy gap. The addition of 15% Li_2CO_3 to PVP/PVA blend films has demonstrated a significant leap that will enhance the ionic conductivity essential for SPEs in Li-ion battery applications and improve overall battery efficiency.

Acknowledgements

Authors express gratitude to the Service Laboratory at the Department of Chemistry, University of Baghdad for their invaluable assistance with FTIR and UV-VIS measurements.

References

[1] T.D. Kusworo et al., "Cellulose Acetate Membrane with Improved Perm-selectivity through Modification Dope Composition and Solvent Evaporation for Water Softening", *Res. J. Appl. Sci. Eng. Technol.*, 7(18) (2014) 3852-3859.

[2] A.P. Echavarría et al., "Fruit juice processing and membrane technology application", *Food Eng. Rev.*, 3 (2011) 136-158.

[3] C.A. Fuenmayor et al., "Filtration of apple juice by nylon nanofibrous membranes", *J. Food Eng.*, 122(1) (2014) 110-116.

[4] E.M. Abdelrazek et al., "Structural, optical, thermal and electrical studies on PVA/PVP blends filled with lithium bromide", *Curr. Appl. Phys.*, 10(2) (2010) 607-613.

[5] D.M. Fernandes et al., "Thermal and photochemical effects on the structure, morphology, thermal and optical properties of PVA/$Ni_{0.04}Zn_{0.96}O$ and PVA/$Fe_{0.03}Zn_{0.97}O$ nanocomposite films", *Polym. Degrad. Stability*, 98(9) (2013) 1862-1868.

[6] C.V.S. Reddy et al., "Dielectric spectroscopy studies on (PVP+PVA) polyblend film", *Microelectron. Eng.*, 83(2) (2006) 281-285.

[7] J. Su et al., "Ferroelectric and piezoelectric properties of nylon 11/poly (vinylidene fluoride) bilaminate films", *J. Polym. Sci. B: Polym. Phys.*, 33(1) (1995) 85-91.

[8] A. Tawansi and H.M. Zidan, "Magnetic effects of the interfacial solitons in polystyrene composites", *J. Phys. D: Appl. Phys.*, 23(10) (1990) 1320.

[9] S. Prasher, M. Kumar and S. Singh, "Electrical and optical properties of O^{6+} ion beam–irradiated polymers", *Int. J. Polym. Anal. Character.*, 19(3) (2014) 204-211.

[10] A. El-Khodary, A.H. Oraby and A.E. Youssef, "The effect of $AgNO_3$ filler on the physical properties of polystyrene films", *Int. J. Mater. Sci.*, 3(1) (2008) 11-24.

[11] M. Abdelaziz, "Cerium (III) doping effects on optical and thermal properties of PVA films", *Physica B: Cond. Matter*, 406(6-7) (2011) 1300-1307.

[12] Z.K. Heiba et al., "Comparative analysis of the optical and electrical properties of PVA/PVP blended polymer with $ZnCo_2O_4$/CdS nanocomposites for optoelectronic and dielectric capacitor applications", *Opt. Mater.*, 150 (2024) 115249.

[13] H.M. Ragab, "Spectroscopic investigations and electrical properties of PVA/PVP blend filled with different concentrations of nickel chloride", *Physica B: Cond. Matter*, 406(20) (2011) 3759-3767.

[14] M.O. Alziyadi et al., "Investigation of the structural, optical dispersion, and optoelectrical characteristics of PVA/PVP/V_2O_5 nanocomposites for optoelectronic devices", *Appl. Phys. A*, 131(1) (2025) 53.

[15] K. Hemalatha, H. Somashekarappa and R. Somashekar, "Micro-structure, AC conductivity and spectroscopic studies of cupric sulphate doped PVA/PVP polymer composites", *Adv. Mater. Phys. Chem.*, 5(10) (2015) 408-418.

[16] I.S. Elashmawi, E.M. Abdelrazek and A.Y. Yassin, "Influence of $NiCl_2$/$CdCl_2$ as mixed filler on structural, thermal and electrical properties of PVA/PVP blend", *Curr. J. Appl. Sci. Technol.*, 4(30) (2014) 4263-4279.

[17] N. Rajeswari et al., "Structural, vibrational, thermal, and electrical properties of PVA/PVP biodegradable polymer blend electrolyte with CH_3COONH_4", *Ionic*, 19(8) (2013) 1105-1113.

[18] K. Sundaramahalingam et al., "Investigations on lithium acetate-doped PVA/PVP solid polymer blend electrolytes", *Polym. Bull.*, 76(11) (2019) 5577-5602.

[19] N.G. Ningappa, A.K. Madikere Raghunatha Reddy and K. Zaghib, "Advanced Polymer Electrolytes in Solid-State Batteries", *Batteries*, 10(12) (2024) 454.

[20] L.P. Teo, M.H. Buraidah and A.K. Arof, "Development on solid polymer electrolytes for electrochemical devices", *Molecules*, 26(21) (2021) 6499.

[21] E.M. Abdelrazek and H.M. Ragab, "Spectroscopic and dielectric study of iodine chloride doped PVA/PVP blend", *Indian J. Phys.*, 89 (2015) 577-585.

[22] N. Rajeswari et al., "A study on polymer blend electrolyte based on PVA/PVP with proton salt", *Polym. Bull.*, 71 (2014) 1061-1080.

[23] S. Konwar et al., "Stable and efficient dye-sensitized solar cells and supercapacitors developed using ionic-liquid-doped biopolymer electrolytes", *Molecules*, 28(13) (2023) 5099.

[24] S. Sheikh and H. Jahromi, "Ionic liquids in green energy storage devices: Lithium-ion batteries, supercapacitors, and solar cells", *Monatshefte für Chemie-Chemical Monthly*, 155(5) (2024) 383-399.

[25] T. Siddaiah et al., "Thermal, structural, optical and electrical properties of PVA/MAA:EA polymer blend filled with different concentrations of Lithium Perchlorate", *J. Sci.: Adv. Mater. Dev.*, 3(4) (2018) 456-463.

[26] M. Fox, **"Optical Properties of Solids"**, 2nd ed., Oxford University Press (2010).

[27] M. Elkattan and M. Gad, "Investigation of the absorption edge and the optical bandgap of PVA/PVP-based thin films", *J. Electron. Mater.*, 54(1) (2025) 831-847.

[28] A. Abu-Jamous, and A.M. Zihlif, "Study of the electrical conduction in poly (ethylene oxide) doped with iodine", *Physica B: Cond. Matter*, 405(13) (2010) 2762-2767.

[29] A.M. El-Naggar et al., "Structural, optical, and electrical parameters of doped PVA/PVP Blend with TPAI or THAI Salt", *Polymers*, 15(12) (2023) 2661.

[30] N.M. Farrage, N.H. Teleb and W.A. Abd El-Ghany, "Investigation of the structural and optical properties of Sb_2S_3/PVA/PVP nanocomposites blended sheets for optoelectronic applications", *Opt. Quantum Electron.*, 56(3) (2024) 488.

[31] M.O. Alziyadi et al., "Structural, linear/non-linear optical, and optoelectrical properties of PVB/Bi_2WO_6 nanocomposite for industrial applications", *J. Thermoplast. Compos. Mater.*, 38(2) (2025) 630-656.

[32] G.D. Cody et al., "Disorder and the optical-absorption edge of hydrogenated amorphous silicon", *Phys. Rev. Lett.*, 47(20) (1981) 1480.

[33] N.F. Mott and E.A. Davis, "Conduction in non-crystalline systems V. Conductivity, optical absorption and photoconductivity in amorphous semiconductors", *Philos. Mag.*, 22(179) (1970) 903-922.

[34] J. Tauc, "Optical properties and electronic structure of amorphous Ge and Si", *Mater. Res. Bull.*, 3(1) (1968) 37-46.

[35] W. Wang et al., "High-temperature piezoelectric conversion using thermally stabilized electrospun polyacrylonitrile membranes", *J. Mater. Chem. A*, 9 (2021) 20395.

[36] M. Abdelaziz and E.M. Abdelrazek, "Effect of dopant mixture on structural, optical and electron spin resonance properties of polyvinyl alcohol", *Physica B: Cond. Matter,* 390(1-2) (2007) 1-9.

[37] C.M. Laot, E. Marand and H.T. Oyama, "Spectroscopic characterization of molecular interdiffusion at a poly(vinyl pyrrolidone)/vinyl ester interface", *Polymer,* 40(5) (1999) 1095-1108.

[38] N. Tian et al., "Reversible reduction of Li_2CO_3", *J. Mater. Chem. A*, 3(27) (2015) 14173-14177.

[39] M.K. Omar and A.H. Ahmad, "Dielectric Properties and Structural Investigation of New Binary Li_2CO_3-LiI Solid Electrolyte", *Int. J. Adv. Eng. Res. Sci.*, 2(1) (2015) 51-55.

[40] H.M. Zidan et al., "Characterization and some physical studies of PVA/PVP filled with MWCNTs", *J. Mater. Res. Technol.*, 8(1) (2019) 904-913.

[41] A.M. El-Mahalawy et al., "Appreciably optimization of PVA/PVP nanocomposite blend for enhanced optoelectronics properties and multifunctional applications", *Physica B: Cond. Matter*, 650 (2023) 414586.

[42] N. Rajeswari et al., "Lithium ion conducting solid polymer blend electrolyte based on bio-degradable polymers", *Bull. Mater. Sci.*, 36 (2013) 333-339.

[43] V.M. Mohan et al., "Electrical properties of poly(vinyl alcohol) (PVA) based on $LiFePO_4$ complex polymer electrolyte films", *J. Polym. Res.*, 17 (2010) 143-150.

[44] J.A. Campbell, A.A. Goodwin and G.P. Simon, "Dielectric relaxation studies of miscible polycarbonate/polyester blends", *Polymer*, 42(10) (2001) 4731-4741.

[45] M.Z. Hamdy et al., "Characterization and some physical studies of PVA/PVP filled with MWCNTs", *J. Mater. Res. Technol.*, 8(1) (2019) 904-913.

[46] Z.M. Dang, Y.H. Zhang and S.C. Tjong, "Dependence of dielectric behavior on the physical property of fillers in the polymer-matrix composites", *Synth. Metals*, 146(1) (2004) 79-84.

[47] A. Jonscher, "The universal dielectric response", *Nature*, 267 (1977) 673-679.

[48] N.A. El-Ghamaz et al., "Conducting polymers VII Effect of doping with iodine on the dielectrical and electrical conduction properties of polyacrylonitrile", *Solid State Sci.*, 24 (2013) 140-146.

[49] R.H. Khudher and A.A. Hasan, "Effect of Lithium Salts on the Optical Properties of PolyAcrylonitrile/Poly Methyl Methacrylate Blends", *Chem. Methodol.*, 6 (2022) 872-885.

[50] R.H. Khudher and A.A. Hasan, "Electrical Properties of PAN/PMMA Blends Doped with Lithium Salts", *Iraqi J. Phys.*, 22(3) (2022) 13-28.

[51] RA. Hasson and A.A. Hasan, "Effect of Metal Oxides Nanoparticles on the Optical Properties of Poly(vinyl chloride)/Poly(vinylidene fluoride) Blends Electrolytes Plasticized with Glycerol", *Iraqi J. Phys.*, 22(2) (2024) 99-103.

[52] R.A. Hasson and A.A. Hasan, "Impact of Incorporating Different Metal Oxide Nanoparticles on Structures and AC Conductivity of PVC/PVDF-based Electrolytes", *Iraqi J. Appl. Phys.*, 20(1) (2024) 133-138.

[53] A.A. Hasan, "Dielectric study of PVC-LiF composites films", *Iraqi J. Sci.*, 62(3) (2021) 861-870.

[54] A.A. Azli, N.S.A. Manan and M.F.Z. Kadir, "Conductivity and Dielectric Studies of Lithium Trifluoromethanesulfonate Doped Polyethylene Oxide-Graphene Oxide Blend Based Electrolytes", *Adv. Mater. Sci. Eng.*, 2015 (2015) article ID 145735, doi: 10.1155/2015/145735.

[55] S.B. Aziz et al., "The Study of Electrical and Electrochemical Properties of Magnesium Ion Conducting CS: PVA Based Polymer Blend Electrolytes: Role of Lattice Energy of Magnesium Salts on EDLC Performance", *Molecules,* 25 (2020) 4503.

[56] M. Ravi et al., "Studies on electrical and dielectric properties of PVP:$KBrO_4$ complexed polymer electrolyte films", *Mater. Chem. Phys.*, 130(1-2) (2011) 442-448.

[57] T. Devika, F.K. Genova and N. Vijaya, "Preparation and characterization of Lithium ion conducting blend polymer (PVA-PVP) with LiBr", *Int. J. Res. Appl. Sci. Eng. Technol.*, 6(3) (2018) 2541-2548.

Table (2) Energy bandgap and optical constants at λ=550nm for 50% PVP :50% PVA blends doped with different lithium salts

Sample	T%	α (cm^{-1})	k	n	ε_r	ε_i	E_g (eV)	E_u (eV)
0	98.08	0.64	2.824E-06	1.231	1.516	6.954E-06	3.80	0.97
15%$LiNO_3$	89.37	3.75	1.640E-05	1.631	2.659	5.350E-05	3.70	1.33
15Li_2CO_3	81.13	6.97	3.052E-05	1.911	3.650	1.166E-04	3.50	1.58
15%LiCl	96.43	1.21	5.311E-06	1.329	1.766	1.411E-05	3.80	1.10
15%$Li_2SO_4.H_2O$	94.06	2.04	8.942E-06	1.442	2.081	2.580E-05	3.70	1.33

